Effect of anomalous warming in the central Pacific on the Australian monsoon

A. S. Taschetto,[1] C. C. Ummenhofer,[1] A. Sen Gupta,[1] and M. H. England[1]

[1] The influence of sea surface temperature (SST) anomalies in the central Pacific Ocean on rainfall variability over Australia is investigated using observations and idealized simulations from an atmospheric general circulation model. We show that the SST warming centered at 180°W is associated with increased monsoon precipitation over northern Australia from January to February and a decrease in December and March over the same region, leading to a shorter and more intense monsoon period. In recent years SST anomalies commonly associated with El Niño events have often exhibited a peak signature in the central, not eastern, Pacific. These so-called El Niño Modoki events are shown here to result in a markedly shorter and more intense Australian monsoon season. **Citation:** Taschetto, A. S., C. C. Ummenhofer, A. Sen Gupta, and M. H. England (2009), Effect of anomalous warming in the central Pacific on the Australian monsoon, *Geophys. Res. Lett.*, *36*, L12704, doi:10.1029/2009GL038416.

1. Introduction

[2] Events related to the recently-termed El Niño Modoki have become more frequent than traditional El Niños over the past few decades [*Ashok et al.*, 2007]. This pattern is characterized by warm SST anomalies in the central Pacific straddled by cold anomalies to either side. The Modoki pattern appears as the second mode of interannual variability in an Empirical Orthogonal Function analysis of monthly SST anomalies from 1979 to 2004, accounting for approximately 12% of the total variance [*Ashok et al.*, 2007]. Any change in the magnitude and location of El Niño-induced SST warming has significant implications for Australian rainfall. For instance, *Wang and Hendon* [2007] showed that the strongest canonical El Niño event of 1997/1998 was associated with near-normal rainfall over Australia, while the modest event of 2002/2003, with a maximum SST warming displaced towards the central equatorial Pacific, experienced near-record drought across the continent. The authors went on to suggest that Australian rainfall is more sensitive to the positive SST anomalies near the date line as opposed to corresponding anomalies in the eastern Pacific. Their study focused on the September to November (SON) months, when El Niño-related impacts are larger over the eastern and southern regions of Australia [*Drosdowsky and Williams*, 1991; *McBride and Nicholls*, 1983]. *Ashok et al.* [2009] report dry conditions over Australia for austral winter (June to August) during the

2004 El Niño Modoki event. *Taschetto and England* [2009] show that the El Niño Modoki pattern is strongly related to Australian droughts during austral autumn (March to May - MAM). The authors reveal that the central Pacific SST warming actually becomes the first coupled mode of variability with Australian rainfall in MAM using a Singular Value Decomposition analysis. On the other hand, correlation analyses between Australian rainfall and El Niño Modoki are not significant for the averaged austral summer season (December to February - DJF). This raises the question of why DJF rainfall does not show a similar response to MAM for the same Modoki signature.

[3] In order to address this question, we examine the monthly, rather than seasonally averaged, evolution of Australian summer rainfall anomalies related to El Niño Modoki events. We show that Modoki affects Australian rainfall differently in summer and autumn, leading to an intensification of rainfall in January and February and a shortening of the active monsoon season over northern Australia. Our findings are confirmed with numerical experiments in an atmospheric general circulation model (AGCM).

2. Data Sets and Model Experiments

[4] In this study we analyze the observed rainfall anomalies in Modoki composite years using the Australian Bureau of Meteorology (BoM) data set [*Lavery et al.*, 1992]. The global SST analysis from the Hadley Centre (HadISST1) [*Rayner et al.*, 2003] was used to composite the years with a Modoki signature. The El Niño Modoki events of 1979/1980, 1986/1987, 1990/1991, 1991/1992, 1992/1993, 1994/1995, 2002/2003 and 2004/2005 were selected according to *Ashok et al.* [2007]. The atmospheric variables of wind speed, specific humidity and vertical velocity were taken from the National Centers for Environmental Prediction/National Center for Atmospheric Research (NCEP/NCAR) Reanalysis [*Kalnay et al.*, 1996]. In addition, we calculate the integrated surface to 500hPa moisture flux and its divergence during Modoki events for both observations and AGCM simulations. We restrict our analyses on the more reliable post-satellite era, i.e., the period after 1979. Model experiments are conducted using the NCAR Community Atmospheric Model (CAM3). The CAM3 has approximately 128 longitudinal by 64 latitudinal points, and 26 vertical levels with a sigma–pressure hybrid coordinate. A complete description of the CAM3 is given by *Collins et al.* [2004].

[5] To assess the sensitivity of Australian rainfall to the location of SST warming, four sets of experiments were conducted forced with climatological monthly SST values and an idealized 1°C positive anomaly superimposed along

[1]Climate Change Research Centre, University of New South Wales, Sydney, New South Wales, Australia.

Rainfall Composite - BoM Data

(a) Dec

(b) Jan

(c) Feb

(d) Mar
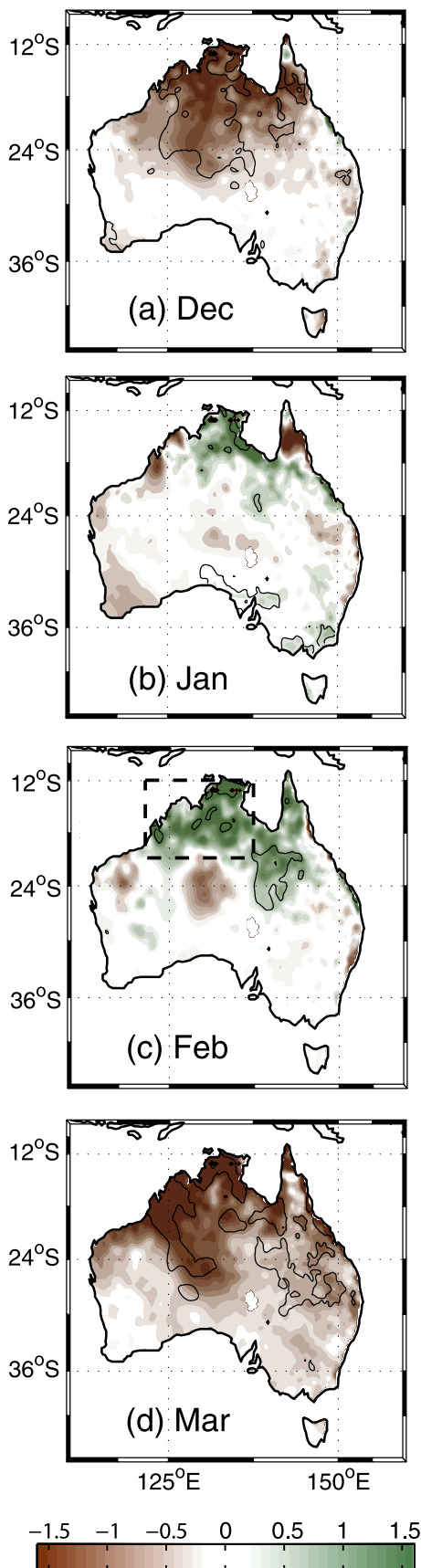
the equatorial Pacific, bounded between 10°N and 10°S and longitudinally located in: (1) the eastern Pacific, from 120°W to 80°W; (2) the central-eastern Pacific, from 160°W to 120°W; (3) the central-western Pacific, from 160°E to 160°W; and, (4) the western Pacific, from 120°E to 160°E. A further experiment was carried out with an idealized Modoki pattern as defined by *Ashok et al.* [2007], with a 1°C warming over the central Pacific at 165°E–140°W, 10°S–10°N, and a 0.5°C cooling on both sides along the equator at 110°W–70°W, 15°S–5°N and 125°E–145°E, 10°S–20°N. To reduce spurious atmospheric circulation driven by sharp gradients at the edges of the SST forcing, a tapering was applied to linearly damp the perturbation to zero over a 10° latitude/longitude band.

[6] Each experiment set consists of an ensemble of 50 members integrated for 12 months. Each integration was started with a slightly different initial atmospheric state to account for the internal variability in the system. As some of the Modoki years co-occur with Indian Ocean Dipole (IOD) events, the forcing of the AGCM with an idealized SST configuration is a valuable approach as it eliminates remote influences that may also affect the Australian monsoon. In particular, the simulated atmosphere in the idealized experiments gives a clear response from only one imposed forcing, i.e., the tropical Pacific warming. The sensitivity experiments were compared to a control run forced by a repeating annual cycle of SST integrated for 80 years.

3. Results

[7] Figure 1 shows composites of observed rainfall anomalies from December to March during El Niño Modoki years. A general decrease in December and March is seen across a large part of the continent while above-normal rainfall takes place over Northern Australia from January to February. The composite anomalies from the CPC Merged Analysis of Precipitation (CMAP) [*Xie and Arkin*, 1997], the NCEP/NCAR and the ECMWF (ERA40) [*Uppala et al.*, 2005] Reanalyses (not shown) are in close agreement with precipitation from BoM, highlighting the robustness of the result. From June to November, Australian rainfall also shows a decrease, but localized over the eastern and southern regions (not shown). The Modoki-related rainfall anomalies are almost the opposite to those seen during traditional El Niños (not shown); with well-below average rainfall over the northwest region during January and February, and neutral conditions during December and March.

[8] To examine the monthly evolution of the Australian monsoon related to Modoki events, we averaged the observed rainfall over the region of northern Australia (12°S–20°S, 120°E–135°E) where the Modoki-related impacts are

Figure 1. (a–d) Rainfall anomaly (mm) composite for Modoki years post-1979 (1979/1980, 1986/1987, 1990/1991, 1991/1992, 1992/1993, 1994/1995, 2002/2003 and 2004/2005). Rainfall anomalies within the dashed box over northwestern Australia (Figure 1c) are averaged to calculate the Australian monsoon index used in Figure 2. Regions within the thin contours are significant at the 90% level.
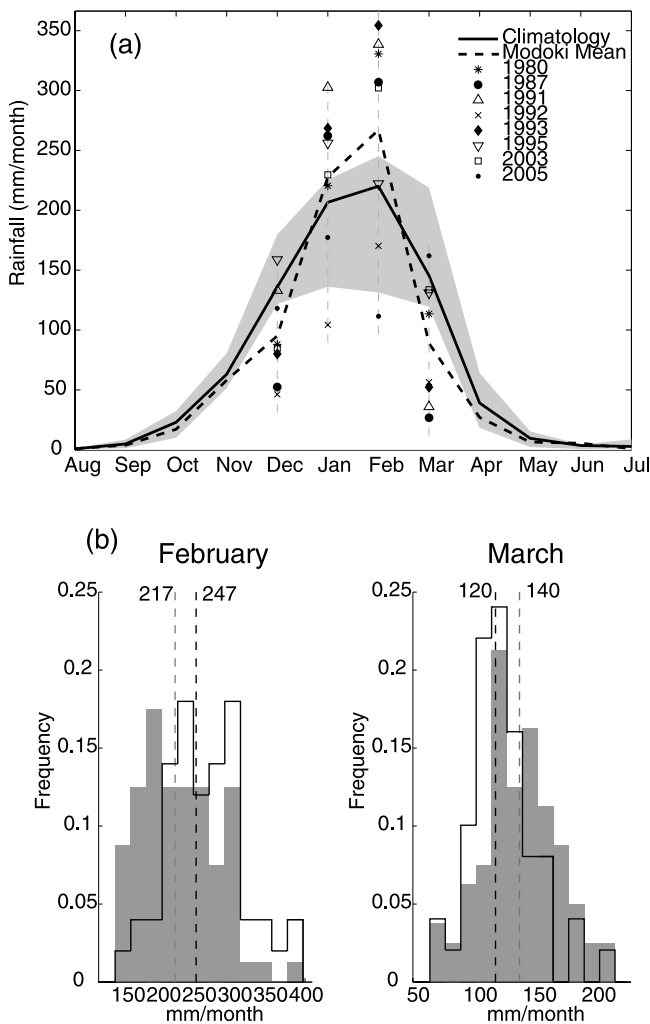
Figure 2. (a) Observed annual cycle of rainfall in northwestern Australia. Black thick line represents the climatology and the thick dashed line indicates the anomalous behavior during El Niño Modoki years. Individual monthly December to March values for Modoki events are highlighted with different symbols. Values outside the grey shaded area are significant at the 95% level based on a Monte Carlo test. (b) Histograms of rainfall for the central-west Pacific warming experiment (dark contour) and the control (grey shaded) in (left) February and (right) March. The dashed lines represent the median rainfall of the control and the perturbation experiments, respectively. The median values (shown above the black dashed lines) of the warming experiment are statistically different at the 95% level from those of the control (grey dashed line), based on both a Student t-test and a Wilcoxon-Rank Sum test.

large and where the annual cycle is characterized by a typical monsoonal regime. The time-series of rainfall averaged over this region is hereinafter referred to as the Australian monsoon index. Figure 2a shows the annual cycle of the Australian monsoon index for Modoki years (dashed line) compared to the long-term climatology (black line). The grey area represents the 95% confidence level for the rainfall climatology based on a Monte Carlo test, i.e., estimated from a distribution of means generated by

randomly choosing eight rainfall observations one thousand times from the entire time-series. A statistically significant decrease in rainfall relative to climatological values is seen in December and March, while a significant increase occurs in January and February. The rate of rainfall decline from February to March is especially strong during El Niño Modoki events (Figure 2a). In this way, the Modoki-related anomalies lead to a shortening of the monsoon season over northern Australia, with an intensification of precipitation in January and February. In other words, Modoki events are associated with a late monsoon onset and an early monsoon termination over Australia.

[9] The observed Modoki-related reduction of precipitation in all months outside January and February is simulated reasonably well in most of the idealized experiments. The strongest rainfall response in February (wet) and March (dry) is seen when the positive SST anomaly forcing is located in the central-west Pacific (see Table 1, bold numbers). This corroborates *Wang and Hendon*'s [2007] finding that Australian climate is sensitive to the location of SST anomalies in the tropical Pacific. In addition, SST warming around the date line, typical of Modoki events, tends to impact more strongly on Australian rainfall than the positive anomalies located in the eastern Pacific, as found during traditional El Niño events. Figure 2b shows the change in the rainfall frequency distributions in the central-west perturbation experiment relative to the control. This suggests that a warming solely in the central-western Pacific may be sufficient to drive the monsoonal changes observed in Modoki years. The rainfall decrease is also simulated in the experiment with a Modoki-like SST pattern, although magnitudes do not change considerably from those with the warming in the central-west Pacific. We thus focus our discussion on the atmospheric response in the central-western Pacific experiment.

[10] In order to assess the causes of the shortening of the Australian monsoon during Modoki years, we calculate the vertically–integrated moisture flux from the surface to 500hPa and the divergence of the moisture flux for both observations and simulations. Figure 3 depicts the observed moisture flux anomalies from February to March composited for Modoki years (Figures 3c–3f) and the corresponding Pacific SST configuration (Figures 3a and 3b).

[11] There are two primary areas where the moisture flux converges, resulting in intensified rainfall in February (Figure 3c): the central-west Pacific and northern Australia. The SST warming in the equatorial Pacific and the relative

Table 1. Simulated Rainfall Anomaly in Northern Australia in Response to an SST Anomaly of 1°C Imposed in the East, Central-East, Central-West and West Pacific Ocean[a]

Experiment	February (mm)	March (mm)	Difference (Feb minus Mar)
East	**23.8**	−5.1	28.9
Central-East	10.8	−1.2	12.0
Central-West	**36.1**	**−13.4**	**49.5**
West	**22.6**	5.6	**17.0**
Modoki	**21.0**	−2.6	**23.6**

[a]Values are shown as anomalies about the mean of the control experimental ensemble set. Bold values indicate significant anomalies at the 95% level using a two-tailed t-test.
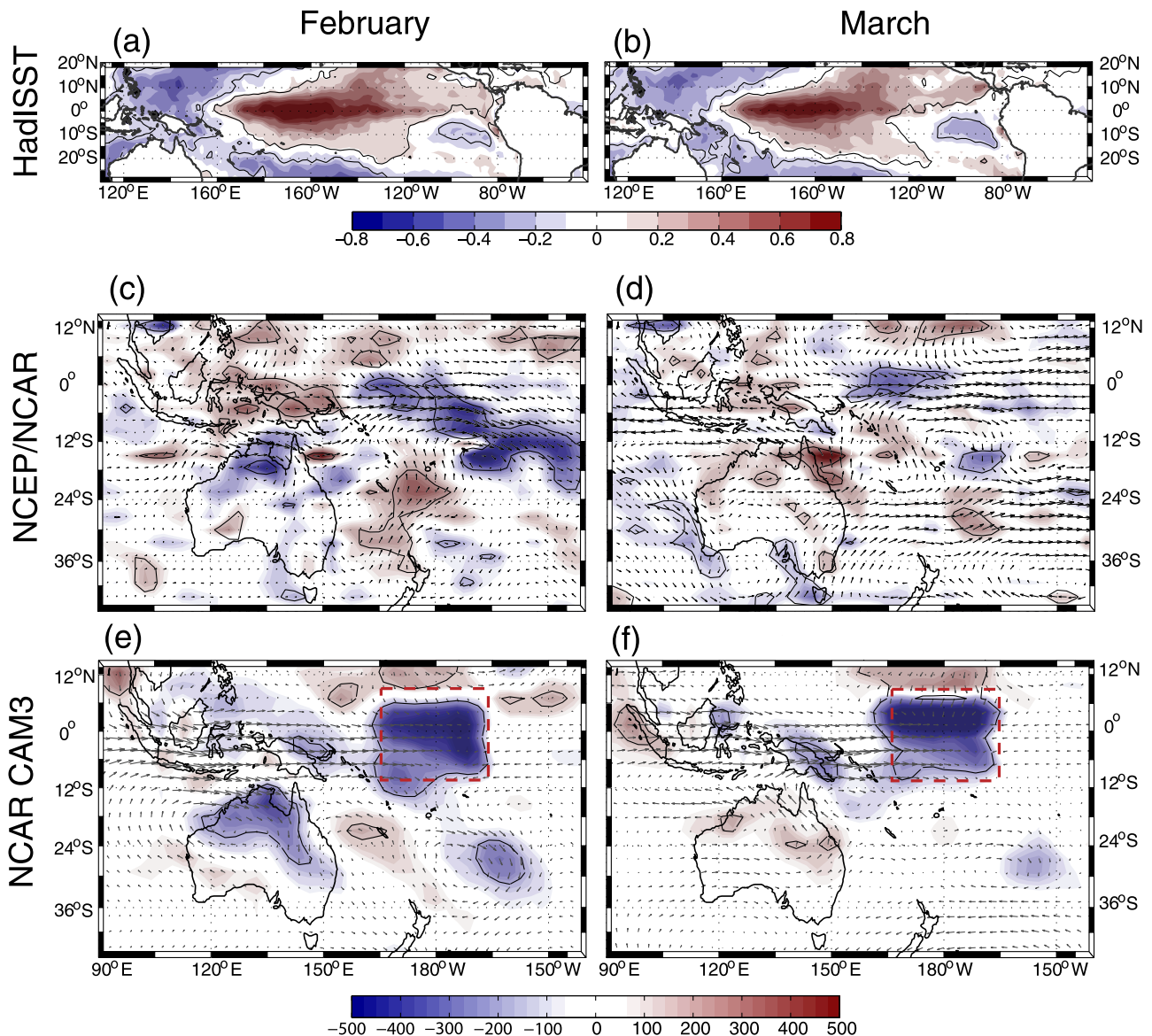
Figure 3. Composites of (a and b) SST anomalies (degrees Celsius), (c and d) moisture flux (vectors, kg m^{-1} s^{-1}) and divergent moisture flux anomalies (shaded, kg s^{-1}) for observations during Modoki events in February (left column) and March (right column). (e and f) Moisture flux and divergent moisture flux anomalies simulated in the central-west Pacific experiment. The maximum vector length is 5 kg m^{-1} s^{-1}. Areas within the thin black contours are significant at the 95% level. The dashed box in Figures 3e and 3f represents the area where the SST anomaly was applied to force the central-west Pacific experiment.

cooling over the Indonesian region in February induces an anomalous pressure gradient that leads to a net moisture flux convergence near 180°W. Northern Australia experiences strong convergence of moisture intensified by an anomalous cyclonic circulation off the northwest coast (Figure 3c).

[12] In March, anomalous divergence of moisture flux is seen over Australia (Figure 3d). This corresponds to less moisture being advected onto the continent and thus less precipitation. The rainfall decrease in March is exacerbated by the subsidence of the western branch of the anomalous Walker circulation that is characteristic of Modoki events (Figure not shown). Anomalous subsidence is not evident over northern Australia in February. This suggests that the advection of moisture plays an important role in modulating the Australian monsoon during Modoki years.

[13] Figures 3e and 3f shows the moisture flux anomalies simulated by the central-west Pacific warming experiment. The model exhibits a similar pattern of anomalous advection of moisture during February as found during observed Modoki years (compare Figures 3c and 3e). This suggests that the SST warming in the central-west Pacific is the key factor in producing increased rainfall over northern Australia during February. The model also simulates below-average rainfall associated with an anomalous divergence of moisture flux over Australia in March (Figure 3f). Again, this reveals

the importance of the central-west Pacific SST anomaly in modulating the Australian monsoon.

4. Discussion and Conclusions

[14] In this study we have shown that the strongest impact of El Niño Modoki on Australian rainfall occurs from austral summer to early autumn, with a shortening and an intensification of the Australian monsoon period. Modoki events are linked to below-normal rainfall across Australia, except between January and February, when positive precipitation anomalies occur in the north. The rainfall decrease in December and the rapid decline in March lead to a late onset and an early termination of the Australian Monsoon season.

[15] The enhanced rainfall in January and February is caused by an anomalous convergence of moisture flux induced by the SST gradient from the warming in the central-west Pacific and the relatively cool SST over the Indonesian region. In March, below-normal rainfall is caused by anomalous divergence of moisture over Australia, and is exacerbated by the subsidence of the western branch of the anomalous Walker Cell typical of Modoki events.

[16] The reason why subsidence does not occur in February but returns in March over Australia remains unclear. It is possible that seasonality may play an essential role in phase-locking the moisture flux in late-summer when the Intertropical Convergence Zone reaches its most southerly position.

[17] The observational results obtained were substantiated using the NCAR CAM3 model forced by idealized SST perturbations. The success of the model in capturing the large−scale features corresponding to the observed Modoki years supports the notion that central-west Pacific SST anomalies drive the shorter and more intense Australian monsoon. These idealized experiments agree with previous findings of *Wang and Hendon* [2007] that Australian rainfall is sensitive to the position of the warming in the Pacific. In particular, for the Australian monsoon, the strongest atmospheric response was obtained when SST anomalies were located around the date line rather than in the east Pacific. These results can potentially improve Australian seasonal forecasting.

References

Ashok, K., S. K. Behera, S. A. Rao, H. Weng, and T. Yamagata (2007), El Nio Modoki and its possible teleconnection, *J. Geophys. Res.*, *112*, C11007, doi:10.1029/2006JC003798.

Ashok, K., S. Iizuka, S. A. Rao, N. H. Saji, and W.-J. Lee (2009), Processes and boreal summer impacts of the 2004 El Niño Modoki: An AGCM study, *Geophys. Res. Lett.*, *36*, L04703, doi:10.1029/2008GL036313.

Collins, W. D., et al. (2004), Description of the NCAR Community Atmosphere Model (CAM 3.0), *NCAR Tech. Note NCAR/TN-464+STR*, 226 pp., Natl. Cent. for Atmos. Res., Boulder, Colo.

Drosdowsky, W., and M. Williams (1991), The Southern Oscillation in the Australian region. Part I: Anomalies at the extremes of the oscillation, *Int. J. Climatol.*, *4*, 619–638.

Kalnay, E., et al. (1996), The NCEP/NCAR 40-year reanalysis project, *Bull. Am. Meteorol. Soc.*, *77*, 437–471.

Lavery, B., A. Kariko, and N. Nicholls (1992), A historical rainfall data set for Australia, *Aust. Meteorol. Mag.*, *40*, 33–39.

McBride, J. L., and N. Nicholls (1983), Seasonal relationships between Australian rainfall and the Southern Oscillation, *Mon. Weather Rev.*, *111*, 1998–2004.

Rayner, N. A., D. E. Parker, E. B. Horton, C. K. Folland, L. V. Alexander, D. P. Rowell, E. C. Kent, and A. Kaplan (2003), Global analyses of sea surface temperature, sea ice, and night marine air temperature since the late nineteenth century, *J. Geophys. Res.*, *108*(D14), 4407, doi:10.1029/2002JD002670.

Taschetto, A. S., and M. H. England (2009), El Niño Modoki impacts on Australian rainfall, *J. Clim.*, *22*, 3167–3174.

Uppala, S., et al. (2005), The ERA-40 re-analysis, *Q. J. R. Meteorol. Soc.*, *131*, 2961–3012, doi:10.1256/qj.04.176.

Wang, G., and H. H. Hendon (2007), Sensitivity of Australian rainfall to inter-El Niño variations, *J. Clim.*, *20*, 4211–4226.

Xie, P., and P. A. Arkin (1997), Global precipitation: A 17-year monthly analysis based on gauge observations, satellite estimates, and numerical model outputs, *Bull. Am. Meteorol. Soc.*, *78*, 2539–2558.

_____

M. H. England, A. Sen Gupta, A. S. Taschetto, and C. C. Ummenhofer, Climate Change Research Centre, University of New South Wales, Sydney, NSW 2052, Australia. (a.taschetto@unsw.edu.au)